



# Classical Pulsators in Gaia DR3

G. Clementini<sup>1,2</sup>

- <sup>1</sup> Istituto Nazionale di Astrofisica – Osservatorio di Astrofisica e Scienza dello Spazio, Via Piero Gobetti 93/3, Bologna, 40129, Italy  
<sup>2</sup> *Gaia* Data Processing and Analysis Consortium (DPAC), Coordination Unit 7 (CU7; Variability Processing)  
e-mail: gisella.clementini@inaf.it

Received: 17 January 2023; Accepted: 26 January 2023

**Abstract.** The last couple of decades have seen a revolution in the field of pulsating stars thanks to the increasing number of ground-based and space-borne facilities that are collecting multi-epoch data over large portions of the sky. A leading role in this revolution is played by *Gaia*, the ESA cornerstone mission that is monitoring the whole celestial sphere since July 2014. On 13 June 2022 the second instalment of the *Gaia* third data release (DR3) published time-series of multi-band photometry, and parameters for about 11 million variable sources. Pulsation is the mechanism driving the light variation in over one third of them. Epoch radial velocities were also released for 1 096 RR Lyrae stars and 799 Cepheids. We review main properties and results for pulsating stars in the *Gaia* DR3, focussing on RR Lyrae stars and Cepheids, in light of the impact they have on the definition of the cosmic distance ladder and the study of the resolved stellar populations in our Galaxy and beyond.

**Key words.** Stars: oscillations – Stars: variables: RR Lyrae – Stars: variables: Cepheids – Methods: data analysis

## 1. Introduction

Since start of operation, in July 2014, the *Gaia* mission is collecting nearly simultaneous astrometry and multi-epoch (spectro)-photometry in three different pass-bands of all sources crossing the CCDs in its focal plane, down to a limiting magnitude  $G \sim 21$  mag, along with spectroscopy of sources brighter than  $G \sim 16.5$  mag. The *Gaia* photometric dataset comprises integrated white-light  $G$ -band photometry covering the wavelength range from 330 to 1050 nm, acquired on the 62 CCDs of the astrometric field (see Fig. 4 in *Gaia* Collaboration et al., 2016), and  $G_{BP}$ ,  $G_{RP}$  spectro-photometry achieved

through low resolution ( $R \sim 20$ -90) blue (BP) and red (RP) prism spectra operating in the wavelength ranges 330-680 nm and 640-1050 nm, respectively, that disperse the light on two arrays of 7 CCDs each. Slitless spectroscopy at a resolution  $R=11,500$  on the calcium triplet (847-874 nm) is then obtained with the Radial Velocity Spectrometer (RVS; Cropper et al., 2018) on board *Gaia*, that disperses the light on 12 specifically dedicated CCDs of the focal plane.

A cyclic, iteratively-improved processing of all the data collected by *Gaia* is performed by dedicated coordination units (CUs) of the *Gaia* Data Processing and Analysis Consortium (DPAC; CU3: astromet-

ric core processing; CU5: photometric processing; CU6: spectroscopic processing; CU4: complex object processing; CU7: variability analysis; and CU8: astrophysical characterization). The *Gaia* mission is producing an unprecedented astrometry (positions, parallaxes and proper motions), multiband photometry reaching 1 mmag precision, and a systematic identification and characterization of tens of different types of variable sources, by monitoring the whole celestial sphere.

*Gaia* data products are published in intermediate data releases, of which the most recent one, the *Gaia* Data Release 3 (DR3; Gaia Collaboration et al., 2022) covering 34 months from 25 July 2014 to 28 May 2017, took place on 13 June 2022. A total number of nearly one trillion CCD measurements of more than 1.8 billions sources were collected for *Gaia* DR3. This enormous amount of data is building up an incremental database that will almost double with *Gaia* DR4, which will publish data products based on 66 months of *Gaia* observations at the end of 2025.

## 2. Identification and processing of *Gaia*'s variable sources

Figure 1 in Gaia Collaboration et al. (2019) provides an overview of different types of variable sources with variability induced either by intrinsic or extrinsic causes. A large number of these variability types can be identified in the *Gaia* data. The variability analysis is applied by the DPAC CU7 to the time-series data of all sources observed by *Gaia*, that is to more than 1.8 billion sources for DR3.

The input dataset of the variability processing for DR3 consisted primarily of calibrated  $G$  and integrated  $G_{BP}$  and  $G_{RP}$  time-series photometry (Riello et al., 2021). The median number of Field-of-View (FoV) photometric measurements per sources was 44, 40 and 41 in  $G$ ,  $G_{BP}$  and  $G_{RP}$  respectively, and reached up to 265 measurements in  $G$  in some specific regions of the sky (see Fig. 1 in Eyer et al., 2022). In addition, the timeseries of RVS radial velocities (Sartoretti et al., 2022) of a subsample of Cepheids and RR Lyrae stars, and the time-series of  $RP$  spectra of long-period

variables (LPVs; Lebzelter et al., 2022) were also analysed. Besides the time-series of photometry, radial velocities and  $RP$  spectra, positions on the sky, parallax, and proper motion are available for the sources from *Gaia* Early Data Release 3 (EDR3; Gaia Collaboration et al., 2021). Figure 3 in Eyer et al. (2022) provides a schematic overview of the various steps for the identification and the subsequent analysis of the DR3 variable sources. Variable sources are identified either by the General Variability Detection (GVD) module, that uses catalogues of known variable stars of different types to train machine learning classifiers (Rimoldini et al., 2022b); or by the Special Variability Detection (SVD) module, that is used to identify some specific types such as candidate planetary transits, short timescale and rotation modulation variables (see Eyer et al., 2017, 2022; Rimoldini et al., 2022b, for details). Candidate variables of different types are then fed to Specific Object Study (SOS) pipelines, that are each tailored for the analysis of a specific variability type.

The total number of variable sources released in DR3 adds to 9.5 million variable stars plus one million variable AGN/QSO. They are subdivided into 24 variability types (and 35 subtypes), 11 of which were validated and further characterized by the SOS pipelines. In addition, 2.5 million galaxies were also identified because of the spurious variability of these extended sources caused by the variation of scan-angle of the observations (Eyer et al., 2022). The following information can be found for these variable sources in the *Gaia* DR3 archive: source identification, multiband time-series  $G$ ,  $G_{BP}$  and  $G_{RP}$  data, along with attributes for the different types (period, peak-to-peak amplitudes, mean magnitudes and colours, etc.) computed by the SOS pipelines and published in the respective `vari_.`(type) tables. We summarize in Table 1 the number of variable stars released in *Gaia* DR3, listing total numbers in the first two rows and number broken down into different types specifically characterized by the SOS pipelines in the remaining 11 rows. The last column of the table provides references to the specific papers describing the general variability processing, the

**Table 1.** Number of variable sources released in *Gaia* DR3 divided per type. Pulsating stars in the classical instability strip are highlighted in boldface.

Type	Number of sources	DR3 table	Ref.
Summary of all-types	$10.5 \times 10^6 + 2.5 \times 10^6$ galaxies	–	(1)
Classification (all-types)	$12.4 \times 10^6$	<code>vari_classifier_result</code>	(2)
AGN	872 228	<code>vari_agn</code>	(3)
<b>Cepheids</b>	<b>15 006</b>	<b><code>vari_cepheid</code></b>	(4)
Compact Companions	6 306	<code>vari_compact_companion</code>	(5)
Eclipsing binaries	2 184 477	<code>vari_eclipsing_binary</code>	(6)
Long-period variables (LPV)	1 720 588	<code>vari_long_period_variable</code>	(7)
Main-Sequence Oscillators	54 476	<code>vari_ms_oscillator</code>	(8)
Microlensing events	363	<code>vari_microlensing</code>	(9)
Planetary transits	214	<code>vari_planetary_transit</code>	(10)
Rotational Modulation	474 026	<code>vari_rotational_modulation</code>	(11)
<b>RR Lyrae stars</b>	<b>270 905</b>	<b><code>vari_rrlyrae</code></b>	(12)
Short-timescale variables	471 679	<code>vari_short_timescale</code>	(13)

**References:** (1)Eyer et al. (2022); (2)Rimoldini et al. (2022b); (3)Carnerero et al. (2022); (4)Ripepi et al. (2022b); (5)Gomel et al. (2022); (6)Mowlavi et al. (2022); (7)Lebzelter et al. (2022); (8)Gaia Collaboration et al. (2022); (9)Wyrzykowski et al. (2022); (10)Panahi et al. (2022); (11)Distefano et al. (2022); (12)Clementini et al. (2022); (13)Eyer et al. (2022, and references therein).

classification into different types, and the validation and analysis performed with the SOS pipelines for 11 DR3 variability types. A full list of the DR3 variability papers is available at <https://www.cosmos.esa.int/web/gaia/dr3-papers>, in the section: Variable Star Classifications and Lightcurves.

### 3. Pulsating stars in *Gaia* DR3

The largest fraction of the variable sources released in *Gaia* DR3 (34%) are pulsating stars. Figure 1 shows, highlighted by white and orange ellipses, the main types of pulsating stars for which specific attributes computed by the SOS pipelines are published in DR3. They can be grouped in three main families that, consistently with their different evolutionary phases, populate three different regions of the Hertzsprung-Russell (HR) diagram: Main Sequence Oscillators, LPVs (low and intermediate-mass stars either on their red giant branch – RGB, or asymptotic giant branch – AGB phases) and variable stars in the

classical instability strip (Horizontal Branch and Blue Loop pulsators).

The Main Sequence Oscillators include  $\beta$  Cepheids, slowly pulsating stars (SPB),  $\gamma$  Doradus stars,  $\delta$  Scuti and SX Phoenicis stars). They are non-radial pulsators of intermediate and high mass stars ( $M \geq 1.3 M_{\odot}$ , spectral types O, B, A, and F) that populate the Main Sequence for luminosities  $\log L/L_{\odot}$  from  $\sim 1$  to  $\sim 4$  (see Fig. 1 of Jeffery & Saio, 2016). Results from the analysis of the DR3 O, B, A, and F main-sequence pulsators, among which in particular the Period–Wesenheit (*PW*) relation defined by 6511  $\delta$  Scuti stars with  $\sigma_{\omega}/\omega < 0.05$ , are presented in Gaia Collaboration et al. (2022).

The family of LPVs gathers Miras, Irregulars, Semi-regulars, and Small Amplitude Red Giant variables. Their luminosity variation is due to single/multi-mode pulsations in radial and non-radial modes, that give rise to multiple, parallel period-luminosity sequences (see e.g. Fig.4 in Trabucchi et al., 2017). The DR3 catalogue of all-sky LPVs (Lebzelter et al., 2022) is the largest to date

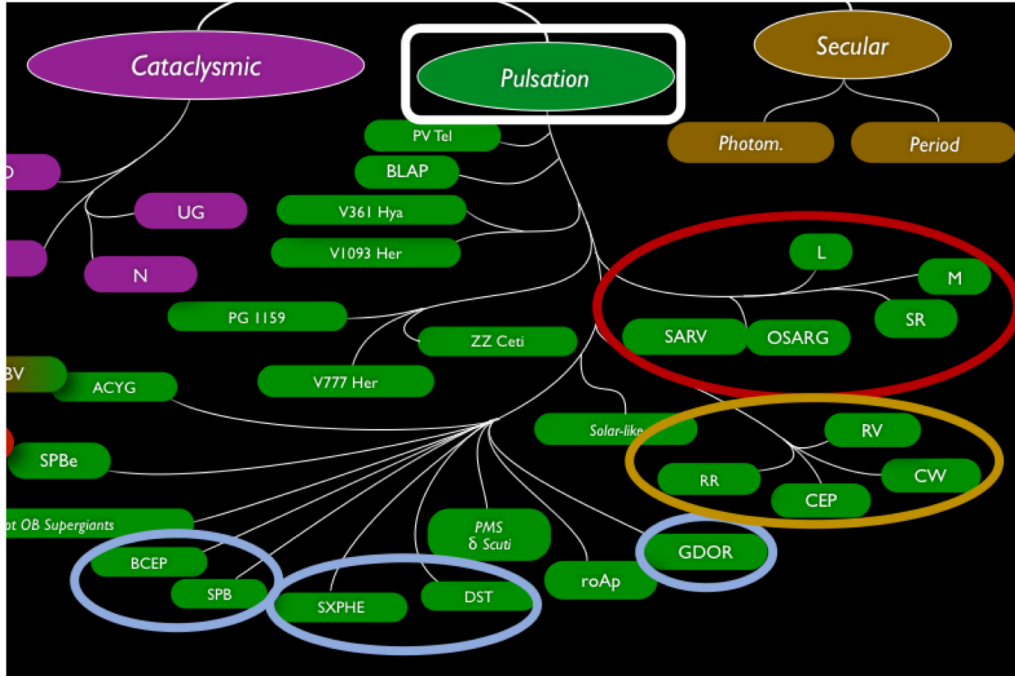


**Fig. 1.** Pulsating stars in the variability tree. In the figure, which is adapted from Fig. 1 of Gaia Collaboration et al. (2019), the light blue, orange and red ellipses highlight three main families of pulsating stars for which specific attributes computed by the SOS pipelines are published in DR3: main-sequence pulsators ( $\beta$  Cepheids – BCEP; slowly pulsating stars – SPB;  $\gamma$  Doradus stars – GDOR;  $\delta$  Scuti – DST, and SX Phoenicis stars – SXPHE); giants in the classical instability strip (RR Lyrae stars – RR; Classical and Anomalous Cepheids – CEP; Type II Cepheids, including W Virgins and BL Herculis types – CW; and RV Tauris – RV); and long-period variables (Irregulars – L; Miras – M; Semi-regulars – SR; and small-amplitude red giants – SARG or OSARG).

with 1 720 558 candidates, periods determined for 392 240 of them, and 546 468 stars classified as Carbon-star candidates based on the profile of their epoch  $RP$  spectra (see Fig. 3 in Lebzelter et al., 2022).

Finally, in the following sections we focus on the pulsating stars that populate the classical instability (RR Lyrae stars and Cepheids of different types) and present the catalogues published for them in *Gaia* DR3.

Cepheid and RR Lyrae candidates identified by the General Supervised Classification of the CU7 variability pipeline (see Fig. 3 in Eyer et al., 2022) are further processed with the SOS Cep&RRL pipeline (Clementini et al., 2016, 2019). Changes and updates of the SOS Cep&RRL pipeline implemented to process the DR3 candidates are described in

Clementini et al. (2022) and Ripepi et al. (2022b). Processing steps performed with the SOS Cep&RRL pipeline are: i) period derivation using the Lomb-Scargle algorithm; ii) non-linear Fourier analysis and modelling of the  $G$ ,  $G_{BP}$ ,  $G_{RP}$ , and RV time-series data; iii) Fourier decomposition of light curves and RV curves; iv) validation of Cepheids and identification of their types/pulsation modes based on period-luminosity ( $PL$ ) and  $PW$  relations calibrated on *Gaia*'s parallaxes; v) validation of RR Lyrae stars and identification of their types/pulsation modes based on period-amplitude and Fourier parameters vs  $P$  relations; and vi) derivation of astrophysical parameters ([Fe/H] metallicities; and  $G$ -absorption –  $A(G)$  values, only for RR Lyrae stars) from the Fourier parameters of the  $G$

light curve. RR Lyrae stars and Cepheids confirmed and validated by the SOS Cep&RRL pipeline (see Clementini et al., 2022; Ripepi et al., 2022b) are referred to as SOS Cepheids and SOS RR Lyrae, hereafter.

### 3.1. Classical pulsators in DR3: the SOS Cepheid sample

The DR3 SOS Cepheids comprise a total number of 15 006 sources with magnitudes between 3.4 and 20.9 in *G*. The sample includes 474 new Cepheids discovered by *Gaia*, and another 327 variable sources with a different classification in the literature that were reclassified as Cepheids (Ripepi et al., 2022b). They are distributed in the MW field and clusters, and in a number of Local Group systems, from the Magellanic Clouds up to the brightest Cepheids in the Andromeda (M31~750 kpc) and Triangulum (M33~ 840 kpc) (Ripepi et al., 2022b) galaxies. They are subdivided into the following types: i) classical Cepheids (DCEPs; 12 554 sources), young, bright ( $M_V$  from  $-2$  to  $-7$  mag) central helium burning Population I giants with typical periods from 0.2 up to 100 d, that can pulsate in the fundamental (F), first-overtone (1O), and second-overtone (2O) modes, or in a combination of them (named Multi in the `vari_cepheid` table); ii) type 2 Cepheids (T2CEPs; 1 902 sources), Population II variable stars that are further subdivided into three different types: BL Herculis (low-mass stars evolving from the blue Horizontal Branch towards the AGB with periods in the range from 1 to 4 d); W Virginis (shell helium-burning low mass AGB stars with periods from 4 to 20 d) and RV Tauri (low-intermediate mass stars evolving off the AGB that pulsate with periods in the range from 20 to 100 d); and iii) anomalous Cepheids (ACEPs; 550 sources), central helium burning low metallicity stars with  $M = 1.2 - 2.6 M_{\odot}$  and  $M_V$  from 0 to  $-2$  mag, that pulsate in F and 1O modes with periods in the range from 0.5 to 2.5 d. Table 2 provides the number of DR3 SOS Cepheids broken down into type, pulsation mode, and parent stellar system. *Gaia*  $G$ ,  $G_{BP}$  and  $G_{RP}$  time-series photometry, for all the SOS Cepheids and RV time-

**Table 2.** Statistics of the DR3 SOS Cepheids (Ripepi et al., 2022b).

Sample	Number
Total	15,006
Known	14 205
Reclassified	327
New discoveries	474
DCEPs F/1O/Multi	7 334/4 857/363
ACEPs F/1O	306/244
T2CEPs BL/WV/RVT	661/935/306
[Fe/H] (F DCEPs, $P < 6.3$ d)	5 265
RV time-series	799
Mean RVs (CU6)	$> 2 000$
LMC region	4 663
SMC region	4 616
All-sky region	5 221
M31	321
M33	185

**Notes:** Accurate metallicities from the RVS spectra, and  $E(B - V)$  values from the *BP/RP* prism spectra obtained by the `gsp_spec` and `gsp_phot` modules of the CU8 APSIS pipeline (Creevey et al., 2022) are also available for  $\sim 7$ -10% of the SOS Cepheids.

series for about 800 of them can be retrieved from the *Gaia* archive. Attributes (period, pulsation mode, intensity-averaged mean magnitudes, amplitudes and Fourier parameters of the light curves and RV curves) computed by the SOS Cep&RRL pipeline are published instead in the `vari_cepheid` table (see Ripepi et al., 2022b, for details).

About 3 400 of the DR3 SOS Cepheids are DCEPs belonging to the MW. This represents the largest and most homogeneous dataset of MW DCEPs published so far. For a thousand of them the DR3 parallaxes have errors  $\sigma_{\varpi}/\varpi < 0.1$  (and  $\text{RUWE} < 1.4$ ), therefore allowing to calibrate with an unprecedented accuracy the DCEP *PL* and *PW* relations and their dependence on metallicity (see e.g. Breuval et al., 2021, 2022; Ripepi et al., 2021, 2022a). These relations are crucial to anchor the first step of the cosmic distance ladder and reduce the uncertainty in the value of the Hubble constant as measured from different distance indicators in

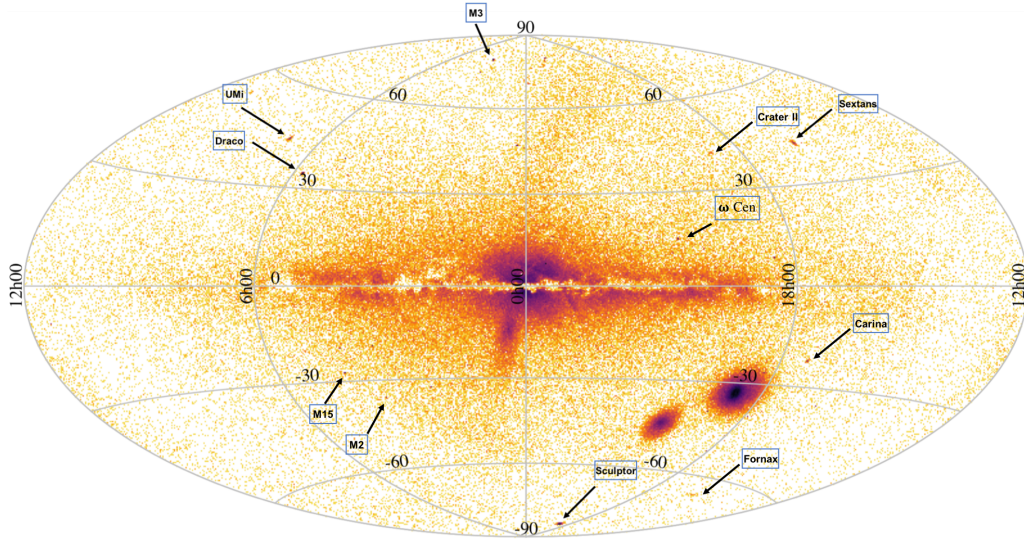


**Fig. 2.** Distribution on the sky of the SOS RR Lyrae stars released in DR3. The two extended RR Lyrae overdensities in the bottom right quadrant of the figure trace the haloes of the Large and Small Magellanic Clouds. The stream of RR Lyrae stars that crosses the Galactic disc is the disrupting Sagittarius dSph galaxy that becomes visible just left below of the centre of the map. Other lower RR Lyrae overdensities can easily be recognised, they correspond to RR Lyrae stars belonging to dSphs and globular clusters (GCs), some of which are labelled.

the local Universe (see e.g. Riess et al., 2021, 2022a,b). Since DCEPs are young stars ( $t \sim 50\text{--}500 \times 10^6$  years), they are preferentially located in regions where star formation is most active. In fact the DR3 DCEPs were successfully used to trace the MW spiral arms (Poggio et al., 2021; Gaia Collaboration et al., 2022), as well as to infer the metallicity gradient in the Galactic disc (Ripepi et al., 2022a; Trentin et al., 2022) and to identify resonance-like features in the Galactic outer disc (Drimmel et al., 2022).

### 3.2. Classical pulsators in DR3: the SOS RR Lyrae sample

The DR3 SOS RR Lyrae comprise a clean sample of 270 905 sources with  $G$ , magnitude between 7.64 and 21.14 mag. Among them 200 294 are RR Lyrae stars already known in the literature and 70 611 are new discoveries from Gaia. The latter are mainly concentrated in the disc and bulge regions of the MW. With typical ages larger than 9-10 bil-

lion years, RR Lyrae stars are excellent tracers of the oldest (Population II) stars in galaxies. They are also standard candles to measure the distance to stellar systems mainly composed by an old stellar population. RR Lyrae stars populate all main Galactic components: disc, bulge and halo. They are abundant in globular clusters (GCs) and are found in all types of galaxies surrounding the MW: Magellanic Clouds, dwarf spheroidal galaxies (dSphs) and ultra-faint dwarfs (UFDs). This is confirmed by the sky distribution of the 270 905 DR3 SOS RR Lyrae shown in Fig. 2. Several RR Lyrae overdensities can clearly be seen, tracing various MW companions, some of which are specifically labelled in the figure. About 1 700 DR3 RR Lyrae stars are concentrated in 95 different GCs in Fig. 2 and more than 1100 are spread among 7 dSph and 16 UFD satellites of the MW. RR Lyrae stars play a crucial role in the identification of the “building blocks” and merging/accretion events that contributed to the build up of the MW halo (see e.g. Catelan & Smith, 2015; Martínez-Vázquez

et al., 2019, and references therein). Table 3 summarises the number of DR3 SOS RR Lyrae broken down into fundamental-mode (RRab), first-overtone mode (RRc), and double-mode RR Lyrae (RRd), and divided into parent stellar systems. The table provides also the number of RR Lyrae for which a photometric metallicity ([Fe/H]) and the absorption in the *G*-band were also computed with SOS Cep&RRL pipeline. *Gaia* *G*, *G<sub>BP</sub>* and *G<sub>RP</sub>* time-series photometry, for all the SOS RR Lyrae and RV time-series for about 1 096 of them can be retrieved from the *Gaia* archive. Attributes (period, pulsation mode, intensity-averaged mean magnitudes, amplitudes and Fourier parameters of the light curves and RV curves, as well as individual [Fe/H] and *A(G)* values computed by the SOS Cep&RRL pipeline are published in the `vari_rrlyrae` table (see Clementini et al., 2022, for details). This is the largest, most homogeneous, and parameter-rich catalogue of all-sky RR Lyrae stars down to *G*  $\sim$  21 mag published so far.

#### 4. Conclusions and future perspectives

The sheer amount of data from the *Gaia* mission represent a gold-mine with applications in many fields of astrophysics. In particular, they have a tremendous impact on aspects of the stellar variability that range from stellar pulsation, to the study of stellar populations, and the distance scale. This is particularly true for Cepheids and RR Lyrae stars, and much more is to come thanks to the longer time baseline and the improved accuracy of the datasets that will be published in the next releases: a Focused Product Release in 2023, DR4 at the end of 2025 with 66 months of data, and DR5 in 2030 containing all data collected by *Gaia* in the 5-year nominal duration of the mission and its extensions. In this same time frame, the spectroscopic surveys planned with the new generation spectrographs WEAVE and 4MOST (see contributions from Battaglia and Chiappini in this conference proceedings) will provide abundances and radial velocities for SOS Cepheids and RR Lyrae stars well beyond the magnitude limit that can be reached by the

**Table 3.** Statistics of the DR3 SOS RR Lyrae stars (Clementini et al., 2022).

Sample	Number
Total	270 905
Known	200 294
New discoveries	70 611
Fundamental mode (RRab)	174 947
First overtone (RRc)	93 952
Double mode (RRd)	2 006
[Fe/H]	133 559
<i>G</i> -absorption ( <i>A(G)</i> )	142 660
RV time-series	1 096
Mean RVs (CU6)	5 096
LMC region	31 379
SMC region	4 788
All-sky region	231 948
95 GCs	1 676
7 dSphs+16 UFDs	1 114

**Notes:** Metallicities from the RVS spectra obtained by the `gesp_spec` module of Apsis are also available for  $\sim$ 200 RR Lyrae stars. Figure 23 in Clementini et al. (2022) shows the good agreement existing between photometric [Fe/H] values from the SOS Cep&RRL pipeline and RVS metallicities from `gesp_spec`.

RVS. This will further enhance the role played by the *Gaia* Cepheids and RR Lyrae stars as primary standard candles for the cosmic distance ladder, as tracers of the different stellar populations in our Galaxy and beyond, and as probes of the Milky Way (MW) structure and assembling process. A strong synergy will also exist with the Legacy Survey of Space and Time (LSST) at the Vera Rubin telescope, that is expected to reach  $\sim$  5 mag fainter than *Gaia* in photometry and  $\sim$  3 mag in astrometry (see Fig. 1 in Ivezić et al., 2015). Finally, the proposal of a new *Gaia*-type mission covering from the optical to the near-infrared (*Gaia*NIR; <https://ui.adsabs.harvard.edu/abs/2021ExA...tm...16H>; <https://doi.org/10.5281/zenodo.7068309>), hence capable to explore the MW most reddened regions is under evaluation by ESA.

**Acknowledgements.** This work presents results from the ESA space mission *Gaia*, processed by

the *Gaia* Data Processing and Analysis Consortium (DPAC). Funding for the DPAC has been provided by national institutions participating in the *Gaia* Multilateral Agreement. In particular, the Italian participation in DPAC has been supported by Istituto Nazionale di Astrofisica (INAF) and the Agenzia Spaziale Italiana (ASI) through grants I/037/08/0, I/058/10/0, 2014-025-R.0, 2014-025-R.1.2015 and 2018-24-HH.0 to INAF (PI M.G. Lattanzi). A special thanks goes to colleagues of the SOS Cep&RRL team, and to the whole CU7 team.

## References

- Breuval, L., Kervella, P., Wielgórski, P., et al. 2021, *ApJ*, 913, 38
- Breuval, L., Riess, A. G., Kervella, P., et al. 2022, *ApJ*, 939, 89
- Carnerero, M. I., Raiteri, C. M., Rimoldini, L., et al. 2022, arXiv:2207.06849
- Catelan, M. & Smith, H. A. 2015, *Pulsating Stars* (Wiley-VCH), 2015
- Clementini, G., Ripepi, V., Leccia, S., et al. 2016, *A&A*, 595, A133
- Clementini, G., Ripepi, V., Molinaro, R., et al. 2019, *A&A*, 622, A60
- Clementini, G., Ripepi, V., Garofalo, A., et al. 2022, arXiv:2206.06278
- Creevey, O. L., Sordo, R., Pailler, F., et al. 2022, arXiv:2206.05864
- Cropper, M., Katz, D., Sartoretti, P., et al. 2018, *A&A*, 616, A5
- Distefano, E., Lanzafame, A. C., Brugaletta, E., et al. 2022, arXiv:2206.05500
- Drimmel, R., Khanna, S., D'Onghia, E., et al. 2022, arXiv:2207.12977
- Eyer, L., Audard, M., Holl, B., et al. 2022, arXiv:2206.06416
- Eyer, L., Mowlavi, N., Evans, D. W., et al. 2017, arXiv:1702.03295
- Gaia Collaboration, Brown, A. G. A., Vallenari, A., Prusti, T., et al. 2021, *A&A*, 649, A1
- Gaia Collaboration, De Ridder, J., Ripepi, V., Aerts, C., et al. 2022, arXiv:2206.06075
- Gaia Collaboration, Drimmel, R., Romero-Gomez, M., et al. 2022, arXiv:2206.06207
- Gaia Collaboration, Eyer, L., Rimoldini, L., Audard, M., et al. 2019, *A&A*, 623, A110
- Gaia Collaboration, Prusti, T., de Bruijne, J. H. J., et al. 2016, *A&A*, 595, A1
- Gaia Collaboration, Vallenari, A., Brown, A. G. A., Prusti, T., et al. 2022, arXiv:2208.00211
- Gomel, R., Mazeh, T., Faigler, S., et al. 2022, arXiv:2206.06032
- Ivezić, Ž., Kahn, S. M., & Eliason, P. 2015, arXiv:1502.06555
- Jeffery, C. S., & Saio, H. 2016, *MNRAS*, 458, 1352
- Lebzelter, T., Mowlavi, N., Lecoeur-Taïbi, I., et al. 2022, arXiv:2206.05745
- Martínez-Vázquez, C. E., Vivas, A. K., Gurevich, M., et al. 2019, *MNRAS*, 490, 2183
- Mowlavi, N., Holl, B., Lecoeur-Taïbi, I., et al. 2022, arXiv:2211.00929
- Panahi A., Zucker S., Clementini G., et al. 2022, *A&A*, 663, A101
- Poggio, E., Drimmel, R., Cantat-Gaudin, T., et al. 2021, *A&A*, 651, A104
- Riello, M., De Angeli, F., Evans, D. W., et al. 2021, *A&A*, 649, A3
- Riess, A. G., Breuval, L., Yuan, W., et al. 2022a, *ApJ*, 938, 36
- Riess, A. G., Casertano, S., Yuan, W., et al. 2021, *ApJ*, 908, L6
- Riess, A. G., Yuan, W., Macri, L. M., et al. 2022b, *ApJ*, 934, L7
- Rimoldini, L., Eyer, L., Audard, M., et al. 2022a, *Gaia DR3 documentation*, European Space Agency; *Gaia Data Processing and Analysis Consortium*.
- Rimoldini, L., Holl, B., Gavras, P., et al. 2022b, arXiv, arXiv:2211.17238
- Ripepi, V., Catanzaro, G., Clementini, G., et al. 2022a, *A&A*, 659, A167
- Ripepi, V., Catanzaro, G., Molinaro, R., et al. 2021, *MNRAS*, 508, 4047
- Ripepi, V., Clementini, G., Molinaro R., et al. 2022b, arXiv:2206.06212
- Sartoretti, P., Blomme, R., David, M., & Seabroke G. 2022, *Gaia DR3 documentation*, European Space Agency; *Gaia Data Processing and Analysis Consortium*
- Trentin, E., Ripepi, V., Catanzaro, G., et al. 2022, arXiv:2209.03792
- Trabucchi, M., Wood, P. R., Montalbán, et al. 2017, *ApJ*, 847, 139
- Wyrzykowski, Ł., Kruszyńska, K., Rybicki K. A., et al. 2022, arXiv:2206.06121